Available online at www.sciencedirect.com
SCIENCE DIRECT®
Virology 318 (2004) 204–213
VIROLOGY
www.elsevier.com/locate/yviro

Genetic and functional analyses of the øX174 DNA binding protein: the effects of substitutions for amino acid residues that spatially organize the two DNA binding domains

Susan L. Hafenstein,[1] Min Chen, and Bentley A. Fane*

Department of Veterinary Sciences and Microbiology, University of Arizona, Tucson, AZ 85721 USA

Received 13 June 2003; returned to author for revision 10 September 2003; accepted 10 September 2003

Abstract

The øX174 DNA binding protein contains two DNA binding domains, containing a series of DNA binding basic amino acids, separated by a proline-rich linker region. Within each DNA binding domain, there is a conserved glycine residue. Glycine and proline residues were mutated and the effects on virion structure were examined. Substitutions for glycine residues yield particles with similar properties to previously characterized mutants with substitutions for DNA binding residues. Both sets of mutations share a common extragenic second-site suppressor, suggesting that the defects caused by the mutant proteins are mechanistically similar. Hence, glycine residues may optimize DNA-protein contacts. The defects conferred by substitutions for proline residues appear to be fundamentally different. The properties of the mutant particles along with the atomic structure of the virion suggest that the proline residues may act to guide the packaged DNA to the adjacent fivefold related asymmetric unit, thus preventing a chaotic packaging arrangement.

Keywords: øX174; Microviridae; DNA binding protein; ssDNA

Introduction

Unlike large icosahedral double-stranded (dsDNA) viruses, in which the packaged genome exists as a dense core within the virion (Earnshaw and Casjens, 1980), single-stranded (ss) DNA and ssRNA genomes are often intimately associated with the inner surface of the capsid protein (Agbandje-Mckenna et al., 1998; Fisher and Johnson, 1993; McKenna et al., 1992, 1994). Altering this association, either by mutating structural proteins or by packaging non-viral nucleic acid, can lead to mature particles with different biophysical characteristics. For example, packaging flock house virus (FHV) with cellular RNA produces a particle with a crystal structure identical to wild-type but with altered solution properties (Bothner et al., 1999). Polymorphic particles result from packaging foreign or incomplete brome mosaic virus (BMV) genomes (Krol et al., 1999). Altering the nucleic acid binding domain of the coat protein prevents viral assembly in BMV (Rao and Grantham, 1996; Sacher and Ahlquist, 1989). Similar phenomena have also been observed with the Microviridae (Hafenstein and Fane, 2002).

As illustrated in Fig. 1, øX174 morphogenesis is dependent on two species of scaffolding proteins and a packaged single-stranded DNA genome (Hafenstein and Fane, 2002; Hayashi et al., 1988). Together, the internal and external scaffolding proteins mediate the assembly of the viral procapsid, into which ssDNA is packaged (Hayashi et al., 1988). After the procapsid is assembled, the single-stranded viral genome is concurrently synthesized and packaged along with the DNA binding protein (J). The C-terminus of protein J, which is highly conserved within the Microviridae, associates with a cleft in the coat protein (F) in each asymmetric unit (McKenna et al., 1992, 1994). The binding of the carboxy tail may allow additional interactions between the genome and a cluster

* Corresponding author. Department of Veterinary Sciences and Microbiology, University of Arizona, Building 90, Tucson, AZ 85721. Fax: +1-520-621-6366.
E-mail address: bfane@u.arizona.edu (B.A. Fane).
[1] Current address: Department of Biological Sciences, Purdue University, West Lafayette, IN 47907, USA.

0042-6822/$ - see front matter © 2003 Elsevier Inc. All rights reserved.
doi:10.1016/j.virol.2003.09.018

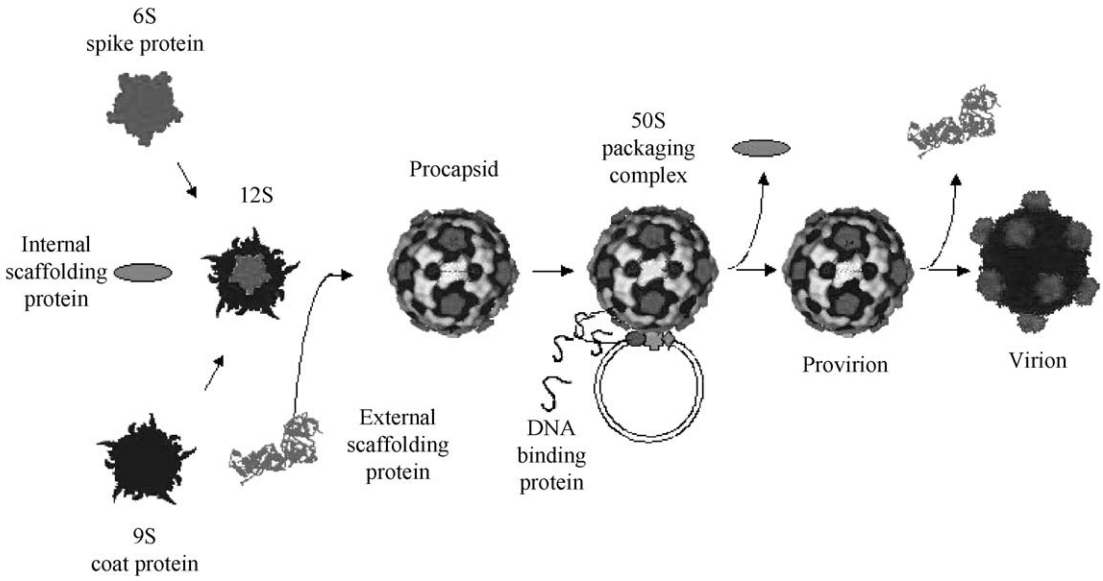

Fig. 1. øX174 morphogenesis.

of nearby basic residues of F. After the initiation of DNA packaging, the internal scaffolding protein (B) dissociates from the interior of the capsid. During the final stages of øX174 morphogenesis, the external scaffolding protein (D) is released, and there is an 8.5-Å radial collapse of coat protein pentamers around the single-stranded genome (Dokland et al., 1997, 1999). High-resolution image reconstruction of a Microviridae procapsid reveals that there are no capsid pentamer–pentamer contacts in the procapsid (Bernal et al., 2003). Hence, the genome, via its tethering to the inner surface of the coat protein, may play a critical role in maintaining the structural integrity of the capsid upon the dissociation of the external scaffolding protein. Altering the genome's association to the inner capsid, or changing the secondary structure of the packaged genome, alters the biophysical characteristics of the mature virion (Hafenstein and Fane, 2002). This suggests that the genome–capsid interactions are performing a scaffolding-like function, mediating the final stages of morphogenesis.

The DNA binding protein is a small (37 amino acids in length), highly basic structural protein that binds the single-stranded DNA genome through nonspecific charge–charge interactions (Dalphin, 1989; Jennings and Fane, 1997). There are two binding regions, one near the amino terminus and one centrally located in the protein (Fig. 2). A spacer region rich in proline residues separates the two binding regions in the øX174 J protein. In order to investigate more fully J protein function during assembly and DNA packaging, the glycine residues within the first and second binding regions and the three proline residues within the spacer region were targeted for analysis. The relative importance of the proline residues has been previously reported (Jennings and Fane, 1997). The glycine residues were chosen because of their conservation within the DNA binding regions of the Microviridae J proteins (Godson et al., 1978, Kodaira et al., 1992; Sanger et al., 1978).

The results of this analysis suggest that the role of the conserved glycine residues may be to optimize the function of the DNA binding motifs. Substitutions for glycine in the binding domain result in biophysically altered particles with properties similar to those observed for particles containing J proteins with substitutions for lysine. Furthermore, the same extragenic second-site suppressors rescue both classes of mutations. On the other hand, the results of biophysical and genetic analyses suggest that the role of the

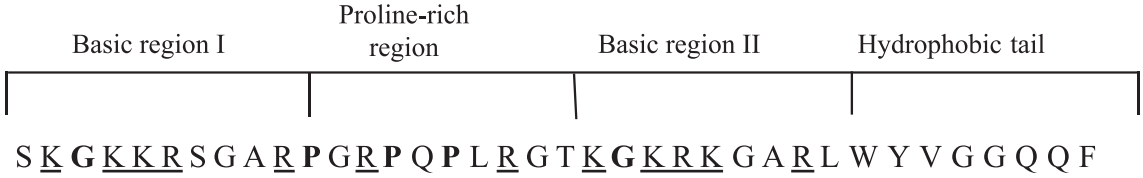

Fig. 2. Primary sequence of protein J, the DNA binding protein. The glycine and proline residues, which are the subject of these studies, are in bold text. Basic residues are underlined. The initial methionine is removed in the mature protein.

Table 1
Efficiency of plating[a] of amber mutants on hosts with informational tRNA suppressors

Mutant	Amino acid substitution								
	Glutamine			Serine			Tyrosine		
	24 °C	33 °C	42 °C	24 °C	33 °C	42 °C	24 °C	33 °C	42 °C
am(J)G3	0.2	0.8	0.7	0.03	0.6	0.5	0.7	1.0	1.0
am(J)G22	RF	1.0	1.0	RF	4.0×10^{-3}	3.0×10^{-4}	4.0×10^{-3}	1.0	1.0
am(J)P16	RF	RF	0.01	RF	RF	0.01	RF	1.0	1.0
am(J)P14	RF	RF	RF	RF	RF	RF	9.0×10^{-4}	1.0	1.0

RF indicates equal to or lower than am^+ reversion frequency.
[a] Restrictive titer/permissive titer, as determined on BAF30 pøXDJ.

proline residues within the spacer region is fundamentally different.

Results

Characterization of substitutions for glycine and proline residues

The conserved glycine codons in the two DNA binding regions, G3 and G22, and two proline codons in the spacer region, P14 and P16, were mutated to amber. Despite repeated attempts, a P11 amber mutant was never recovered. Missense proteins were generated by propagating mutants in hosts with tRNA informational suppressors. Serine, glutamine, and tyrosine substitutions for G3 appear to be fairly well tolerated, conferring, at most, weak cold sensitive (*cs*) phenotypes (Table 1). However, substitutions for G22, located in the second DNA binding region, result in strong *cs* or lethal phenotypes. A similar phenotypic phenomenon was observed in previous studies in which lysine residues in both DNA binding domains were altered (Jennings and Fane, 1997). Substitutions for proline residues resulted in predominately lethal phenotypes.

Characterization of infectious particles packaged with mutant DNA binding proteins

To further assess the biophysical characteristics of particles containing missense J proteins, G3 → Q and G22 → Q particles were analyzed by buoyant density centrifugation. In these experiments, mutant particles were analyzed in the same gradient with wild type. Particles were differentially titered as described in the figure legend (Fig. 3, panel A). As with previously documented particles packaged with charge-reduced J proteins (Hafenstein and Fane, 2002), G22 → Q particles are more dense than wild type, suggesting that the nature of the defect in the DNA binding domains may be similar. Several hypotheses can explain this increased density (see Discussion, and below).

The G3 → Q substitution produces two types of packaged particles, one with near wild-type density and another

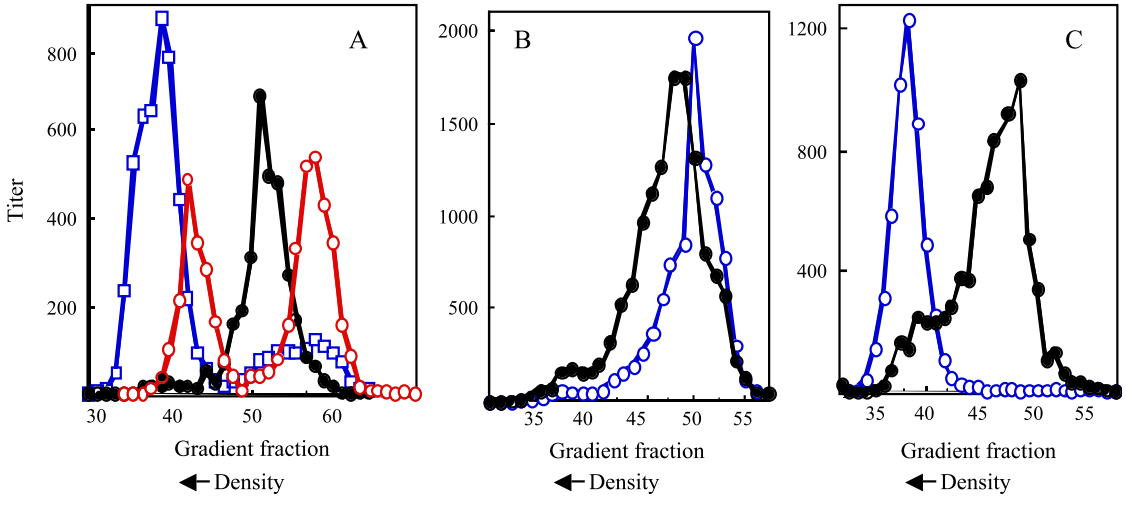

Fig. 3. Buoyant densities of wild type and particles generated with missense proteins. Both particles were analyzed in the same gradient. An additional genetic marker, *amB*, was placed in the wild type background. This allowed the particles to be differentially titered on BAF30 pøXB at 33 °C. The titer of the amber J mutants was determined on BAF30 pøXDJ at 33 °C. In each panel, particle titers (*y*-axes) have been normalized relative to each other for the purpose of graphing. Panel A: symbols: *am(J)G22* with the missense G → Q protein, open square; wild-type phage, closed circle; and *am(J)G3* with missense G → Q protein, open circle. Panels B and C: *am(J)G3*, particles packaged with the missense J protein, G3 → Q, heavy and light peaks were harvested and assayed again with wild type.

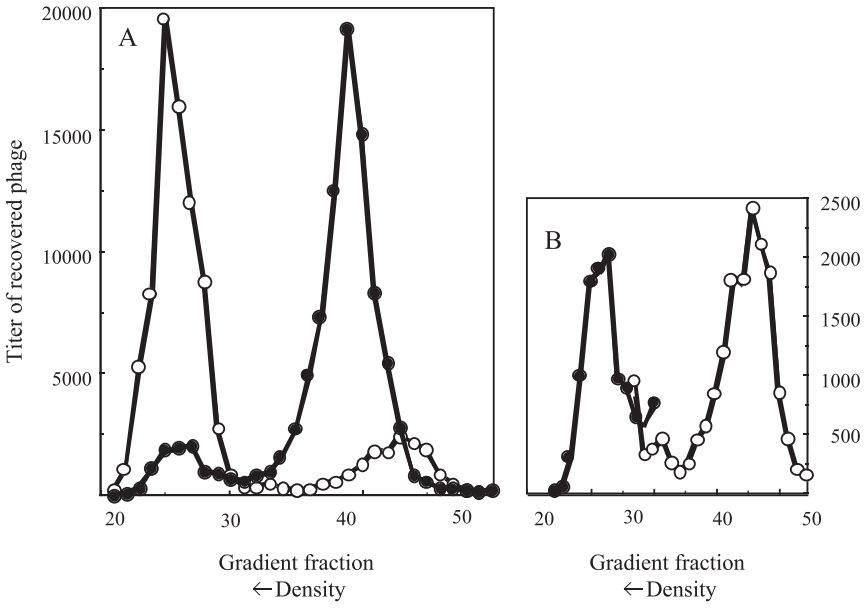

Fig. 4. Reinvestigation of G22 → Q particles and wild type using higher titers. Particles were differentially titered as described in the legend of Fig. 3. Symbols: wild type, closed circles; mutant particles, open circles. Panel A: total particle counts. Panel B: enlargement to illustrate subpopulations.

significantly denser. When each particle type was harvested and assayed in a second gradient, the densities remained constant, suggesting that particles did not interconvert (Fig. 3, panels B and C). To determine whether multiple particle types, which may have been below the level of detection in the experiment presented in Fig. 3, also exist among G22 → Q and wild-type populations, the assay was repeated with higher titers. A second population of mutant G22 → Q particles less dense than wild type was visualized, and a significant minor peak was also seen for wild-type virion (Fig. 4, panels A and B). Since both density populations are observed with both wild-type and mutant particles, it suggests that the DNA binding protein causes a ratio shift between extant particles, as opposed to creating entirely novel structures.

Particles packaged with the J P14 → Y and J P16 → S proteins are less dense than wild type (Fig. 5, panel A, P16 → S, data not shown). This is in contrast to serine substitutions for glycine residues, which resulted in particles with increased densities. Although these results suggest that density differences are not the consequence of lower intracellular J protein concentrations caused by informational suppressors, which are known to operate at reduced efficiencies (Winston et al., 1979), this possibility was directly

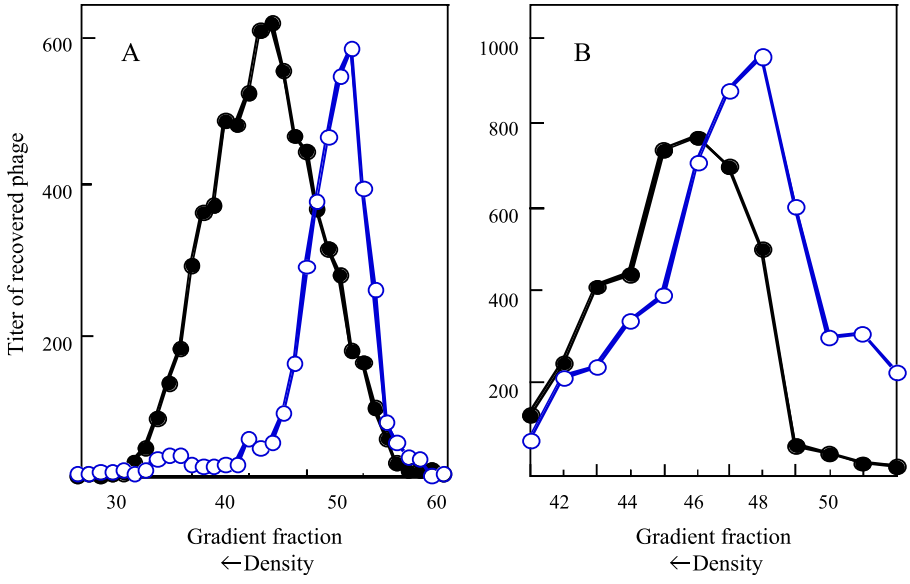

Fig. 5. Buoyant density gradients of proline mutants. Symbols: wild type, closed circles; mutant, open circles. Panel A: *am(J)P14* → Y, tyrosine insertion. Panel B: *cs(J)P16L*.

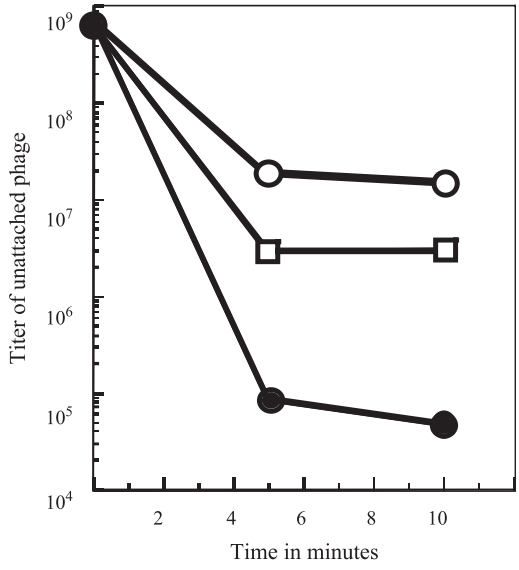

Fig. 6. Attachment assays. Symbols: wild type, closed circles; *amJG22* with glutamine missense protein, open boxes; *cs(J)P16L*, open circles.

examined by repeating the assay using a *cs* P16 *missense* mutation (Fig. 5, panel B). Again the resulting particles were less dense than wild type.

Host cell attachment as an assay for differences on the outer surface of the capsid

Since host cell attachment is a function of the capsid's outer surface, attachment assays were used to explore possible structural differences (Fig. 6). The attachment efficiency of wild-type particles is three orders of magnitude greater than that of the mutant particles with substitutions for proline and glycine residues (Fig. 6). All three curves reach a plateau within 5 min. It is not known if there are any differences in initial attachment rates. Similar results were obtained for the other mutants tested, suggesting that alterations to the surface of the capsid are produced by a mutant internal protein.

Second-site genetic analyses

To explore further the role of the conserved glycine residues in the DNA binding regions, second-site suppressors of the missense proteins were isolated (Table 2). Using *am(J)G22* as the parental strain, second-site suppressors were selected for their ability to suppress defects associated with glutamine substitutions at 24 °C and serine substitutions at 42 °C (see Material and methods). Putative second-site suppressor mutants were identified by the retention of the amber phenotype, J protein complementation-dependent growth, and verified by a direct DNA sequence analysis. All second-site suppressing mutations were extragenic, conferring amino acid substitutions in the coat protein (F). The *su(J)-F T204I* mutation was independently recovered three times. It was also used in series of marker rescue experiments to verify the identity of the suppressing amino acid (see below).

The *su(J)/am(J)G22* double mutants were assayed for ability to grow as a function of temperature and missense insertion (Table 2). Suppressors isolated at 42 °C only suppress defects associated with G → S substitutions, whereas one of the suppressors isolated at 24 °C *su(J)-F T204I* suppress *ts* defects and *cs* defects associated with any missense substitution. This suggests that reduced temperatures represent a more restrictive growth condition and selects for suppressors with stronger phenotypes. No suppressors were recovered for *am(J)G3*, *am(J)P14*, and *am(J)P16* due to either leaky phenotypes or high *am* reversion frequencies.

To determine whether the isolated suppressors were both necessary and sufficient to confer the suppressing pheno-

Table 2
Efficiency of plating of *su(J)/amG22* mutants on hosts with informational tRNA suppressors

Mutant[a]	Amino acid substitution								
	Glutamine			Serine			Tyrosine		
	24 °C	33 °C	42 °C	24 °C	33 °C	42 °C	24 °C	33 °C	42 °C
Parental mutant									
am(J)G22	RF[b]	1.0	1.0	RF	4.0×10^{-3}	3.0×10^{-4}	4.0×10^{-3}	1.0	1.0
With suppressor									
Su(J)-F L94I	RF[b]	1.0	1.0	RF	**1.0**	1.0	RF	1.0	1.0
Su(J)-F T5A	RF	1.0	1.0	RF	**1.0**	1.0	RF	RF	1.0
Su(J)-F Q80H	RF	0.9	1.0	RF	**0.5**	0.8	RF	1.0	1.0
Su(J)-F V71F	1.0	1.0	1.0	RF	**1.0**	RF	**1.0**	1.0	1.0
Su(J)-F T204I	1.0	1.0	1.0	RF	**1.0**	**1.0**	**1.0**	1.0	1.0
Su(J)-F G22C	1.0	1.0	RF	RF	**1.0**	RF	**1.0**	1.0	RF

Underlined text indicates the conditions of isolation. Text in boldface indicates conditions at which the suppressor mutant is viable but the parent mutant is restricted.

[a] Suppressors are named as follows, "-F" indicates the gene in which the suppressor resides, the major coat protein. "L94I", a leucine to isoleucine substitution for amino acid 94.

[b] Restrictive titer/permissive titer, as determined on BAF30 pøXDJ. RF indicates equal to or lower than am^+ reversion frequency.

Table 3
Recombination rescue by a cloned second-site suppressor[a]

Mutant	Restrictive plating efficiencies[b]			
	sup D host with plasmid	*sup D* host with no plasmid	*sup°* host with plasmid	*sup°* host[c] with no plasmid
am(J)G22	0.1	5.0×10^{-5}		5.0×10^{-5}
am(J)P14	1.0×10^{-4}	1.0×10^{-4}		1.0×10^{-4}
$J^{-}3K \rightarrow LII$[d]			5.0×10^{-3}	4.0×10^{-4}
$J^{-}3K\&R \rightarrow LI$			8.0×10^{-5}	2.0×10^{-4}

[a] Restrictive titer/permissive titer, as determined on BAF30 pøXDJ.
[b] Experiments with amber mutants and $J^{-}3K\&R \rightarrow LI$ were performed at 33 °C. The experiments with $J^{-}3K \rightarrow LII$ were performed at 42 °C.
[c] For amber mutants, this value represents the am^{+} reversion frequency. For $J^{-}3K \rightarrow LII$ and $J^{-}3K\&R \rightarrow LI$, this value represents the lethal phenotype reversion frequency.
[d] In $J^{-}3K \rightarrow LII$, the three lysine residues in the second DNA binding domain have been changed to leucine residues. Similarly, in $J^{-}3K\&R \rightarrow LI$, three lysine residues and one arginine residue have been changed to leucine residues in the first DNA binding domain.

type, a series of recombination rescue experiments were performed. Four hundred nucleotides surrounding the *su(J)-F T204I* mutation were cloned into a non-expression Topo vector and the plasmid placed into the C122 (*sup°*) and BAF7 (*sup D*) cell lines. Rescue frequencies for parental mutants were calculated under restrictive conditions. The *am(J)G22* parent was rescued in BAF7(*sup D*) at 42 °C (Table 3). The presence of both parental and suppressing mutations in the recombinants was verified via a direct sequence analysis. Rescue experiments were also performed with the *am(J)P14* mutant and two previously isolated mutants, $J^{-}3K\&R \rightarrow LI$ and $J^{-}3K \rightarrow LII$, which contain substitutions for lysine residues in the first and second DNA binding regions (see footnote b, Table 3). No rescue was observed.

Cross-functional second-site suppressors as an assay for common molecular defects

The charge-reduced mutants resulting from substitutions for lysine residues and the glycine substitution mutants share common biophysical characteristics. To determine whether this is the consequence of similar molecular defects, a previously characterized extragenic second-site suppressor of lysine substitutions, *su(J)-F S1F*, was built directly into the *am(J)G3* and *am(J)G22* backgrounds. In both cases, the mutation suppressed defects associated with glycine substitutions (Table 4), suggesting that the substitutions in the DNA binding region confer similar mechanistic defects. The *su(J)-F S1F* suppressor was previously shown to have no effect on substitutions for proline residues (Jennings and Fane, 1997). The inability of the *su(J)-F T204I* suppressor to rescue the $J^{-}3K \rightarrow LII$ mutant is probably due to the relative severity of this particular mutation. Unlike substitutions for glycine residues, the $J^{-}3K \rightarrow LII$ substitutions confer a dominant lethal phenotype, for which the *su(J)-F S1F* mutation was originally selected to suppress. The *su(J)-F T204* suppressor, on the other hand, was selected to suppress a much less severe phenotype.

Discussion

Interactions between the viral genome and structural proteins have been shown to be essential to virion assembly in several single-stranded RNA plant viruses (Lee and Hacker, 2001; Rao and Grantham, 1996; Rossmann et al., 1983; Sacher and Ahlquist, 1989) and insect viruses (Dong et al., 1998; Wery et al., 1994). In the dsRNA infectious bursal disease virus, the binding of the two genomic segments by a highly basic region of the C-terminal tail of VP3 appears to be key to the organization of protein and RNA during morphogenesis (Tacken et al., 2002). In addition, the packaged genome appears to stabilize the mature viral particle in the dsDNA papillomavirus (Fligge et al., 2001) as well as in many of the ssRNA plant viruses (Da Poian et al., 2002; Willits et al., 2003). In the Microviridae, where the single-stranded DNA genome is tethered to the inner surface of the capsid at each asymmetric unit via protein interactions, alterations to either the protein or the DNA component of the tether can change the biophysical properties of the resulting virion (Hafenstein and Fane, 2002). Clearly genomic material may function as a structural component in virion morphogenesis.

Table 4
Efficiency of plating[a] of *su(J)-F S1F/am(J)* mutants on hosts with informational tRNA suppressors

Mutant	Amino acid substitution								
	Glutamine			Serine			Tyrosine		
	24 °C	33 °C	42 °C	24 °C	33 °C	42 °C	24 °C	33 °C	42 °C
am(J)G3	0.2	0.8	0.7	0.03	0.6	0.5	0.7	1.0	1.0
With suppressor	**1.0**	1.0	1.0	**1.0**	1.0	1.0	1.0	1.0	1.0
am(J)G22	RF	1.0	1.0	RF	4.0×10^{-3}	3.0×10^{-4}	4.0×10^{-3}	1.0	1.0
With suppressor	RF	1.0	1.0	RF	**1.0**	**1.0**	RF	1.0	1.0

Bold text indicates conditions at which the suppressor mutant is viable but the parent mutant is restricted.
RF indicates equal to or lower than am^{+} reversion frequency.
[a] Restrictive titer/permissive titer, as determined on BAF30 pøXDJ.

Altered densities: substitutions for glycine residues may interfere with DNA binding ability of the J protein

G3 and G22 are components of the two highly conserved DNA binding motifs. Substitutions for either of these glycine residues result in particles with buoyant densities greater than wild type, a phenomenon similar to that observed for charge-reduced mutants with decreased DNA binding ability (Hafenstein and Fane, 2002). Several hypotheses can explain the density differences. Alterations in the number of molecules of J protein found in the final particles could be compensated by internally retained or displaced cesium counter ions. The contribution of the Cs^+ ions was assessed to be minimal in previous studies with charge-altered mutants (Hafenstein and Fane, 2002). In those studies, as in these, it was possible to produce two types of mutant particles containing the same mutant DNA binding protein either with or without extragenic suppressors. Differences in buoyant densities were detected by analyzing both particle types in the same gradient. Two discernable peaks were present, separated by at least eight fractions. Similar experiments were conducted with particles containing substitutions for glycine residues (suppressors for substitutions of proline residues could not be isolated). While the presence of the suppressor appeared to shift the density of particles toward a wild-type value, separations of the parental and double mutant, assayed in the same gradient, were always less than two fractions (data not shown). Therefore, possible counter ion effects cannot be ruled out experimentally with the same degree of rigor as could be done in Hafenstein and Fane (2002).

However, variation in the amount of protein and counter ions incorporated per virion would result in a density curve visualized as broad peak, stretching away in a continuous curve toward heavier and lighter densities values until particles were no longer viable (detection in these assays required viability). However, this was not the experimental result. Mutant particles with substitutions for G3 segregated into two distinct and sharp density peaks. Substitutions at G22 result in a density pattern similar to wild type, consisting of a major density population and accompanied by a minor population. These results suggest that the final stages of morphogenesis may not consist of one pathway, but several parallel pathways, influenced by the packaged genome.

Substitutions for glycine and proline residues most likely confer mechanistically different defects

Substitutions for glycine residues result in particles with biophysical properties similar to those of the previously reported charge-reduced J mutants with substitutions for lysine residues (Hafenstein and Fane, 2002). Furthermore, the suppressor of the charge-reduced mutants also suppresses the defects associated with missense substitution for both glycine residues, suggesting that the two classes of mutations are mechanistically similar.

While it seems likely that glycine mutants disrupt the DNA binding capability of J protein, proline mutants appear to be disrupting a different function of protein J. Particles formed with proline-substituted proteins have unique biophysical properties not shared by other mutant particles. Unlike substitutions for lysine residues, where there may be a redundancy of function in the DNA binding regions, and glycine residues that may serve to optimize interactions between lysine residues and the genome's phosphate backbone, proline substitutions are tolerated poorly, with most substitutions conferring lethal phenotypes. In addition, proline substitutions are not rescued by the extragenic suppressors of charge-reduced J mutants (Jennings and Fane, 1997). In the atomic structure of the virion (McKenna et al., 1992, 1994), the C-terminus of protein J lodges in an internal cleft of the viral capsid protein (F). The central part of the protein traces a path toward the fivefold axis of symmetry. The N-terminus is located in the adjacent asymmetric unit, near the C-terminus binding cleft, which would be occupied by another J protein (Fig. 7). Considering their location within the J protein, the proline residues may function to guide the DNA to the adjacent fivefold related asymmetric unit, resulting in wild-type genomic organization.

Speculative models for the final stages of virion morphogenesis

Unlike most dsDNA viruses, the øX174 genome, as with other single-stranded viruses, does not exist as a dense core in the mature virion (Agbandje-Mckenna et al., 1998; Chen et al., 1989; McKenna et al., 1992, 1994). Instead, it is tethered to the capsid's inner surface by the highly basic DNA binding protein (J) and a group of basic capsid amino acid residues. Accordingly, between 8% and 10% of the genome is ordered in the X-ray structure (McKenna et al., 1992, 1994). However, this arrangement does not reflect the secondary structure of naked øX174 DNA, which is substantially richer in secondary structure than packaged DNA (Benevides et al., 1991). Therefore, it is likely that the genome's association with the inner surface of the capsid constrains the formation of genomic secondary structure.

Within the procapsid, there are no discernable pentamer–pentamer interactions (Bernal et al., 2003). The integrity of the particles appears to be maintained by the scaffolding proteins. After packaging, the internal scaffolding protein is extruded from the structure and replaced by the DNA binding protein and the tethered genome. This may supplant scaffolding function in the provirion. The provirion to virion transition is marked by the release of the external scaffolding protein and the completion of the 8.5-Å radial collapse of coat protein pentamers (Bernal et al., 2003; Dokland et al., 1997, 1999). In the mature virion, numerous F–F contacts occur across the twofold axes symmetry (McKenna et al., 1992, 1994).

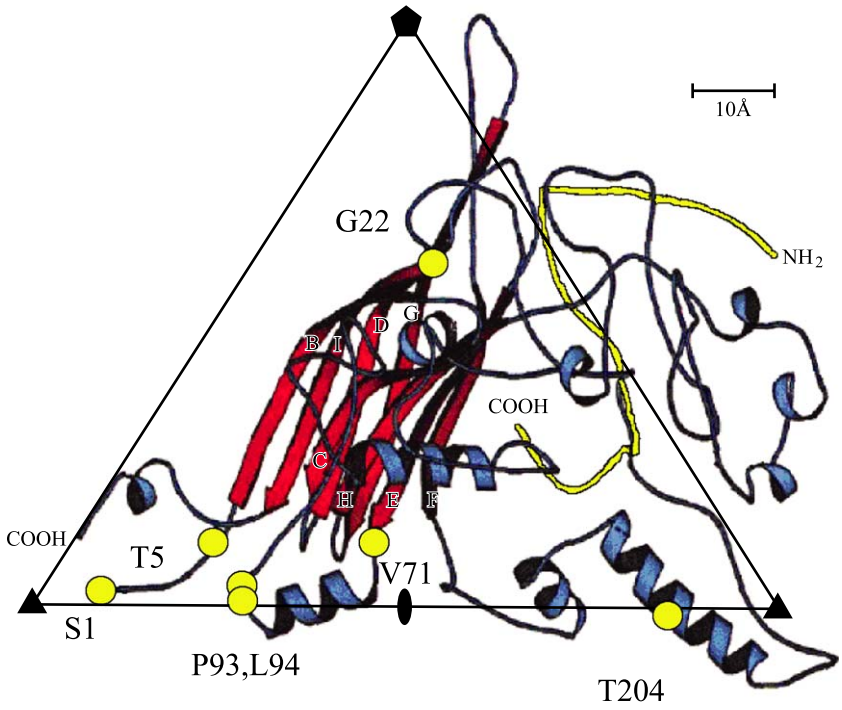

Fig. 7. Location of the second-site suppressors of missense substitutions for G22. The øX174 coat protein is depicted in red and blue. The DNA binding protein is depicted in yellow. The suppressors are identified by yellow circles. Twofold, threefold, and fivefold axes of symmetry are marked with oval, triangles, and pentagon, respectively. Modified from McKenna et al. (1992, 1994).

The location of the second-site suppressors described here suggests a model for the final stages of morphogenesis. All but one of the suppressing mutations map to what would be the twofold axes of symmetry in the capsid. The exception, F G22 C, is a substitution at the tip of a β strand, β-B, which might cause the β strand to shift toward the twofold axis of symmetry (Fig. 7). As the external scaffolding proteins dissociate from the provirion, coat protein pentamers are no longer constrained and would begin to associate across the twofold axes of symmetry. The genome's propensity to form secondary structure may mediate the inward movement of the pentamers. Hence, altering its association with the inner surface capsid would lead to either a smaller or larger collapse, producing altered particles. The second-site suppressors would restore the proper degree of inward movement. In this model, capsid alterations would be evenly distributed and icosahedrally ordered. However, this model may require too much uniformity throughout the entire maturing particle, which may be inconsistent with an evolutionary dynamic system and experimental observations. For example, øX174 can be packaged with foreign DNA as long as the 30 base pair origin of replication is present (Hafenstein and Fane, 2002). While such particles exhibit altered properties, they are infective. Alternatively, the chemical composition of the genome may have simply evolved not to interfere with the final stages of morphogenesis, as opposed to mediating it. In this model, altering protein–DNA interactions would not initially affect the structure of associating pentamers. However, as the mutant particle matures, misplaced DNA may create a distortion preventing the correct conformation, but only at the last twofold axes of symmetry to form during the final stage of the maturation process. The second-site suppressors, in turn, would then correct the distortions at the altered axes.

Materials and methods

Phage plating, stock preparation, media, phage purification, bacterial strains, cloned genes, buoyant density, native gel migration, and attachment assays

The plating protocols, media, and stock preparation have all been previously described (Fane and Hayashi, 1991). *Escherichia coli* C strain C122 (*sup*°) is the wild-type host; BAF5, BAF7, and BAF8 contain a *sup E*, *sup D*, and *sup F* informational suppressor, respectively. BAF30 is a *recA* derivative of C122 (Fane et al., 1992). Plasmids pøXB and pøXDJ contain isopropyl β-D-thiogalactopyranoside (IPTG)-inducible clones of the øX174 genes designated (Burch and Fane, 2000; Burch et al., 1999). The *slyD* host mutation confers resistance to øX174 E-protein-mediated cell lysis (Roof et al., 1994). Buoyant density, native gel migration, and attachment assays have been previously described (Hafenstein and Fane, 2002).

Phage mutants

The øX174 mutants, *J⁻3K&R → LI*, *J⁻3K → LII*, and *su(J)-F S1F* have been previously described (Hafenstein and Fane, 2002, Jennings and Fane, 1997). *J⁻* amber mutations were constructed by oligonucleotide-mediated mutagenesis designed to introduce amber codons at the selected sites (Fane et al., 1992). BAF30 pøXDJ cells were transfected with mutagenized DNA and incubated at 33 °C until plaques appeared. Plaques were stabbed into C122 and pøXDJ seeded lawns. Putative mutants were identified by complementation-dependent growth then verified by direct DNA sequence analysis. The *su(J)-F S1F* was built directly into the *am(J)G3* and *am(J)G22* backgrounds by oligonucleotide-mediated mutagenesis. Putative double mutants were identified by rescue of the parental *cs* or *ts* phenotype on the *sup D* host and retention of the amber phenotype. Genotypes were verified by direct DNA sequence analysis.

Isolation of second-site suppressors

The *am(J)G22* mutant was used for the isolation of second-site suppressors. The second-site suppressors were selected for their ability to suppress defects associated with serine insertion at 42 °C and glutamine insertion at 24 °C. Viable phage (5.0×10^6) were plated under restrictive conditions. Revertant plaques were stabbed into three indicator lawns; one seeded with the restrictive host at nonpermissive temperatures, C122 (*sup°*), and BAF30 pøXDJ. Putative suppressor mutants were identified by retention of the *am(J)* phenotype and growth under restrictive conditions. All genotypes were verified by direct DNA sequence analysis.

Recombination rescue experiments

øX174 DNA containing 400 nucleotides surrounding the *su(J)-F T204I* mutation was amplified via PCR. The DNA was cloned into a non-expression Topo 2.1 vector (Invitrogen) and transformed into the C122 (*sup°*) and BAF7 (*sup D*) cell lines. Rescue frequencies for parental mutants were calculated under restrictive conditions, and the presence of both the parental and suppressing mutations in the recombinants were verified via a direct sequence analysis.

Acknowledgment

This research was supported by an NSF Grant (MCB0234976) to B.A. Fane.

References

Agbandje-McKenna, M., Llamas-Saiz, A.L., Wang, F., Tattersall, P., Rossmann, M.G., 1998. Functional implications of the structure of the murine parvovirus, minute virus of mice. Structure 6, 1369–1381.

Benevides, J.M., Stow, P.L., Ilag, L.L., Incardona, N.L., Thomas Jr., G.L., 1991. Differences in secondary structure between packaged and unpackaged single-stranded DNA of bacteriophage øX174 determined by Raman spectroscopy: a model for øX174 DNA packaging. Biochemistry 30, 4855–4862.

Bernal, R.A., Hafenstein, S., Olson, N.H., Bowman, V.D., Chipman, P.R., Baker, T.S., Fane, B.A., Rossmann, M.G., 2003. Structural studies of bacteriophage alpha3 assembly. J. Mol. Biol. 325, 11–24.

Bothner, B., Schneemann, A., Marshall, D., Reddy, V., Johnson, J.E., Siuzdak, G., 1999. Crystallographically identical virus capsids display different properties in solution. Nat. Struct. Biol. 6, 114–116.

Burch, A.D., Fane, B.A., 2000. Foreign and chimeric external scaffolding proteins as inhibitors of Microviridae morphogenesis. J. Virol. 74, 9347–9352.

Burch, A.D., Ta, J., Fane, B.A., 1999. Cross-functional analysis of the Microviridae internal scaffolding protein. J. Mol. Biol. 286, 95–104.

Chen, Z.G., Stauffacher, C., Li, Y., Schmidt, T., Bomu, W., Kamer, G., Shanks, M., Lomonossoff, G., Johnson, J.E., 1989. Protein–RNA interactions in an icosahedral virus at 3.0 A resolution. Science 245, 154–159.

Dalphin, M.E., 1989. Bacteriophage øX174: crosslinking studies of the virion and prohead and biophysical characterization of the gene J protein. Doctoral thesis, University of California, San Diego.

Da Poian, A.T., Johnson, J.E., Silva, J.L., 2002. Protein–RNA interactions and virus stability as probed by the dynamics of tryptophan side chains. J. Biol. Chem. 49, 47596–47602.

Dokland, T., McKenna, R., Ilag, L.L., Bowen, B.R., Incardona, N.L., Fane, B.A., Rossmann, M.G., 1997. Structure of a viral assembly intermediate with molecular scaffolding. Nature 389, 308–313.

Dokland, T., Bernal, R.A., Burch, A., Pletnev, S., Fane, B.A., Rossmann, M.G., 1999. The role of scaffolding proteins in the assembly of the small single-stranded DNA virus øX174. J. Mol. Biol. 288, 595–608.

Dong, X.F., Natarajan, P., Tihova, M., Johnson, J.E., Schneemann, A., 1998. Particle polymorphism caused by deletion of a peptide molecular switch in a quasi-equivalent icosahedral virus. J. Virol. 72, 6024–6033.

Earnshaw, W.C., Casjens, S.R., 1980. DNA packaging by the double-stranded DNA bacteriophages. Cell 21, 319–331 (Review).

Fane, B.A., Hayashi, M., 1991. Second-site suppressors of a cold-sensitive prohead accessory protein of bacteriophage øX174. Genetics 128, 663–671.

Fane, B.A., Head, S., Hayashi, M., 1992. The functional relationship between the J proteins of bacteriophages øX174 and G4 during phage morphogenesis. J. Bacteriol. 174, 2717–2719.

Fisher, A.J., Johnson, J.E., 1993. Ordered duplex RNA controls capsid architecture in an icosahedral animal virus. Nature 361, 176–179.

Fligge, C., Schafer, F., Selinka, H.C., Sapp, C., Sapp, M., 2001. DNA-induced structural changes in the papillomavirus capsid. J. Virol. 75, 7727–7731.

Godson, G.N., Barrell, B.G., Standen, R., Fiddes, J.C., 1978. Nucleotide sequence of bacteriophage G4 DNA. Nature 276, 236–247.

Hafenstein, S., Fane, B.A., 2002. øX174 genome–capsid interactions influence the biophysical properties of the virion: evidence for a scaffolding-like function for the genome during the final stages of morphogenesis. J. Virol. 76, 5350–5356.

Hayashi, M., Aoyama, A., Richardson, D.L., Hayashi, M.N., 1988. Biology of the bacteriophage øX174. In: Calendar, R. (Ed.), The Bacteriophages, vol. 2. Plenum, New York, pp. 1–71.

Jennings, B., Fane, B.A., 1997. Genetic analysis of the øX174 DNA binding protein. Virology 227, 370–377.

Kodaira, K., Nakano, K., Okada, S., Taketo, A., 1992. Nucleotide sequence of the genome of bacteriophage α3: interrelationship of the genome structure and the gene products with those of the phages øX174 G4 and øK. Biochim. Biophys. Acta 1130, 277–288.

Krol, M.A., Olson, N.H., Tate, J., Johnson, J.E., Baker, T.S., Ahlquist, P.,

1999. RNA-controlled polymorphism in the in vivo assembly of 180-subunit and 120-subunit virions from a single capsid protein. Proc. Natl. Acad. Sci. U.S.A. 96, 13650–13655.

Lee, S.K., Hacker, D.L., 2001. In vitro analysis of an RNA binding site within the N-terminal 30 amino acids of the southern cowpea mosaic virus coat protein. Virology 286, 317–327.

McKenna, R., Olson, N.H., Chipman, P.R., Baker, T.S., Booth, T.F., Christensen, H., Aasted, B., Fox, J.M., Bloom, M.E., Wolfinbarger, J.B., Agbandje-McKenna, M., 1992. Atomic structure of single-stranded DNA bacteriophage øX174 and its functional implications. Nature 355, 137–143.

McKenna, R., Ilag, L.L., Rossmann, M.G., 1994. Analysis of the single-stranded DNA bacteriophage øX174 at a resolution of 3.0 Å. J. Mol. Biol. 237, 517–543.

Rao, A.L., Grantham, G.L., 1996. Molecular studies on bromovirus capsid protein: II. Functional analysis of the amino-terminal arginine-rich motif and its role in encapsidation, movement, and pathology. Virology 226, 294–305.

Roof, W.D., Horne, S.M., Young, K.D., Young, R., 1994. *slyD*, a host gene required for phi X174 lysis, is related to the FK506-binding protein family of peptidyl-prolyl *cis-trans*-isomerases. J. Biol. Chem. 269, 2902–2910.

Rossmann, M.G., Abad-Zapatero, C., Erickson, J.W., Savithri, H.S., 1983. RNA-protein interactions in some small plant viruses. J. Biomol. Struct. Dyn. 1, 565–579.

Sacher, R., Ahlquist, P., 1989. Effects of deletions in the N-terminal basic arm of brome mosaic virus coat protein on RNA packaging and systemic infection. J. Virol. 63, 4545–4552.

Sanger, F., Coulson, A.R., Friedmann, C.T., Air, G.M., Barrell, B.G., Brown, N.L., Fiddes, J.C., Hutchison III, C.A., Slocombe, P.M., Smith, M., 1978. The nucleotide sequence of bacteriophage øX174. J. Mol. Biol. 125, 225–246.

Tacken, M.G., Peeters, B.P., Thomas, A.A., Rottier, P.J., Boot, H.J., 2002. Infectious bursal disease virus capsid protein VP3 interacts both with VP1, the RNA-dependent RNA polymerase, and with viral double-stranded RNA. J. Virol. 76, 11301–11311.

Wery, J.P., Reddy, V.S., Hosur, M.V., Johnson, J.E., 1994. The refined three-dimensional structure of an insect virus at 2.8 A resolution. J. Mol. Biol. 235, 565–586.

Willits, D., Zhao, X., Olson, N., Baker, T.S., Zlotnick, A., Johnson, J.E., Douglas, T., Young, M.J., 2003. Effects of the cowpea chlorotic mottle bromovirus beta-hexamer structure on virion assembly. Virology 306, 280–288.

Winston, F., Botstein, D., Miller, J.H., 1979. Characterization of amber and ochre suppressors in Salmonella typhimurium. J. Bacteriol. 137, 433–439.